Supporting Information

Post-synthetic modulation of UiO-66-NH_2 with cobaloxime catalyst for efficient hydrogen production

Saddam Sk,[ab] Sandip Prabhakar Shelake,[bc] Dependu Dolui,[d] Suhana Karim,[d] Rajib Ghosh,[e] M. V. Jyothirmai,[f] Annadanam V. Sesha Sainath,[bc] Ujjwal Pal*[ab] and Arnab Dutta*[dg]

[a] Department of Energy & Environmental Engineering, CSIR-Indian Institute of Chemical Technology, Hyderabad-500007, India.
[b] Academy of Scientific and Innovative Research (AcSIR), Ghaziabad-201002, India.
[c] Polymers and Functional Materials and Fluoro-Agrochemicals Department, CSIR-Indian Institute of Chemical Technology, Hyderabad-500007, India.
[d] Chemistry Department, Indian Institute of Technology Bombay, Powai, Mumbai-400076, India.
[e] Radiation & Photochemistry Division, Bhabha Atomic Research Centre, Mumbai-400085, India
[f] Department of Chemical Engineering, Indian Institute of Technology Kanpur, Kanpur-208016, India.
[g] Interdisciplinary Programme in Climate Studies, Indian Institute of Technology Bombay, Powai, Mumbai-400076, India.

*Corresponding author: arnab.dutta@iitb.ac.in (A. Dutta), upal03@gmail.com & ujjwalpal@iict.res.in (U. Pal)

Materials and Experimental details

Materials and reagents

All the reagents are purchased from commercially available sources and used as such without any further purification: N, N-Dimethylformamide (DMF, Finar Chemicals), Zirconium (IV) tetrachloride ($ZrCl_4$, Sigma-Aldrich), 2-(Cyclohexylamino)ethane sulfonic acid (CHES, >99% Titration, Sigma-Aldrich), MES hydrate (>99.5%, Titration, Sigma-Aldrich), 2-Aminoterephthalic acid (NH_2-BDC, Sigma-Aldrich), glacial acetic acid (CH_3COOH, Finar Chemicals), Methanol (MeOH, Finar Chemicals), Ethanol (EtOH), 4-pyridinecarboxaldehyde (4-PC), Acetone (CH_3COCH_3), Sodium borohydride ($NaBH_4$), Chloroform ($CHCl_3$), Acetonitrile (CH_3CN). In all the experiments distilled water (DI H_2O) was used. The complex Co(dimethylglyoxime)$_2Cl_2$ was synthesized according to the previously reported literature.[1]

Preparation of Catalyst

Preparation of UiO-66-NH_2

It is prepared through a facile solvothermal treatment.[2] Typically, 5 mL DMF solution of $ZrCl_4$ (10.20 mg, 8.75 mM), and 5 mL DMF solution of NH_2-BDC (14.50 mg, 8.01 mM) were mixed in small RB. Following that, 1.2 mL CH_3COOH was added, and then transferred into a Teflon liner stainless-steel autoclave. The autoclave was sealed and heated at 120 °C for 12 h. The product was collected by centrifugation and washed three times with DMF, and then sequentially immersed in MeOH for three 24 h periods. Finally, NH_2-UiO-66 was activated by removing the solvent under vacuum for 12 h at 50 °C.

Preparation of UiO-66-N=CH-4-Pyr (A)

0.150 g (0.085 mmol) of UiO-66-NH_2 was dispersed in EtOH (15 mL) in 50 mL RB by sonication for 10 mins. Then 144 µL of 4-PC was added to the dispersion at room temperature and stirring for 5 min and then heated this reaction mixture at 60 °C for 24 hours under N_2 atmosphere. The resulting reaction mixture was precipitated by centrifugation at 6000 rpm for 5 mins. This process was repeated four times and the final product was washed 3 times with CH_3COCH_3 and centrifuged again at 6000 rpm. The yellow coloured solid dried for 12 hours at 85 °C.

Preparation of UiO-66-NH-CH_2-4-Pyr (A')

50 mg (0.0269 mmol) UiO-66-N=CH-4-Pyr (A) was taken in 10 mL of absolute EtOH, cooled to 0 °C prior to slow drop wise addition of $NaBH_4$ (20 mg, 0.5286 mmol) dissolved in 5 mL

cold H_2O. The reduction was completed within 30 minutes as monitored via thin layer chromatography (TLC). After that, the reaction mixture was stirred at room temperature for another half an hour. The reaction mixture dried under reduced pressure to obtain a solid yellowish white product. The obtained product dried under 65 °C for 12 hours.

Preparation of Co-UiO [A' with complex Co(dimethylglyoxime)$_2$Cl$_2$]

25 mg (0.0688 mmol) Co(dimethylglyoxime)$_2$Cl$_2$ was taken in a 50 mL RB Flask. 15 mL of $CHCl_3$ was added to the solution, and it was sonicated for 5 min. 50 mg (0.0269 mmol) A' was added to this suspension and stirred under N_2 for 10 min. Then 2 mL of CH_3CN was added to this mixture and stirred at RT. After 30 min of stirring 2 mL, dry EtOH added and immediate formation of a brown precipitate was observed. The stirring was continued for another 30 minutes and then the precipitate filtered. The precipitate washed with $CHCl_3$ and cold ethanol and dried under reduced pressure.

Characterizations

The chemical structures of synthesized samples were confirmed by ^{1}H- and ^{13}C-NMR (AVANCE-400 or INOVA-500) spectral techniques using 570 µL of 40% HF solution in DMSO-d_6 with tetramethyl silane as internal standard. FTIR spectroscopy was used to characterize the surface feature of the particles. The spectra were acquired using a Perkin Elmer FTIR spectrometer. The structural phase analysis of the as-synthesized photocatalysts was performed by using Powder X-ray diffraction patterns (XRD) on a Bruker AXS diffractometer (D8 advance) at a generator voltage of 40 kV and current of 30 mA using Cu-Kα_1 irradiation (λ = 1.5406 Å). The sample was scanned in the range of 2θ = 10-80° with a scan rate of 1 s/step. X-ray photoelectron spectroscopy (XPS) was performed via a Kratos (axis 165) analytical instrument with Mg Kα irradiation. About 10^{-9} Torr pressure was maintained in the spectrometer. Transmission electron microscopy (TEM) image of the representative photocatalysts was obtained by using a JEOL 2010EX TEM instrument equipped with the high-resolution style objective-lens pole piece at an acceleration voltage of 200 kV fitted with a CCD camera. N_2 adsorption-desorption isotherms of the photocatalysts were obtained on a Quantachrome Nova 2200e gas adsorption analyzer at 77 K. Thermogravimetric analyses (TGA) of the samples were carried out using the TA Instruments SDT Q600 apparatus to study the thermal treatment. Around 12-15 mg of the sample was placed in the TG pan and was heated at a scan rate of 10 °C min^{-1} within a temperature range of 25 to 900 °C and under an inert atmosphere of N_2 gas flow of 50 ml min^{-1}. The optical properties were characterized by

using UV-Vis diffuse reflectance spectroscopy (DRS) Perkin Elmer Lambda 750 instrument using $BaSO_4$ as a reference. The sample has been placed in the sample holder for the measurement and the light is allowed to pass through the sample which leads to the absorption of the light and the light transmitted by the sample has been recorded. The Photoluminescence (PL) spectra were recorded using a Fluorolog-3 spectrofluorometer (Spex model, JobinYvon) at their respective excitation (λ_{ex}) wavelength. Fluorescence Lifetime decay measurements were carried out by using time-correlated single photon counting (TCSPC) setup (Fluorolog-3 Triple Illuminator, IBH Horiba Jobin Yvon). Briefly, the samples were excited at 380 nm, and the emission was observed at 420 nm. Inductively coupled plasma-optical emission spectroscopy (ICP-OES) was carried out using a Perkin-Elmer ICP-OES chemical analyzer. The sample was first dissolved in aqua regia at 70 °C for 30 min. Then, the solution was transferred and diluted to 100 ml in the volumetric flask. Finally, the obtained solution was analysed on the ICP-OES.

Table S1. Structural parameters obtained from N_2 adsorption isotherms analysis:

Samples	S_{BET} (m^2 g^{-1})[a]	Pore volume (cm^3 g^{-1})[b]	Average pore size (nm)[b]
UiO-66-NH_2	295.5	0.25	3.37
Co-UiO	13.3	0.006	17.74

a. Obtained from BET method.
b. Total pore volume taken from the N_2 adsorption volume at a relative pressure (P/P_0) of 0.99.

Computational details

The three-parameter compound of Becke with Lee-Yang-Parr (B3LYP) function[3] is employed using Gaussian 09 program package[4] to perform density functional theory (DFT) calculations. The 6-31G* basis set (B3LYP/6-31G) is incorporated to fully optimize all structures without any constraint. For modelling the molecules, we used Avogadro software[5] which is an open-source molecule builder.

Electrocatalytic hydrogen generation experiment

The working electrodes were prepared via drop casting on a precleaned dried Carbon Paper (CP). Typically, a piece of Carbon Paper (CP) with a dimension of 0.5 x 0.5 cm with a geometrical surface area of 0.25 cm^2 was considered unless otherwise mentioned. The catalytic ink of the samples was prepared by sonicating (30 min. in an ultrasonic bath) 3 mg of the

catalyst in 230 µL absolute ethanol and 20 µL Nafion (5 wt% from Sigma Aldrich). After that, 20 µL of prepared catalytic ink was drop cast on CP via micropipette and dried at room temperature. 0.96 mg/cm^2 is the approximate catalyst loading. Further, these catalyst-modified working electrodes were used in 0.1 M respective buffers for the HER study (pH 5-7: MES buffer, pH 8-9: CHES buffer).

Electrochemical studies for H_2 evolution reaction were measured by performing cyclic voltammetry (CV), linear sweep voltammetry (LSV) and chronoamperometry using a computer-controlled AUTO LAB PGSTAT-204 potentiostat. All the electrochemical experiments were measured by a conventional three-electrode setup containing Ag/AgCl (3M in KCl) as a reference electrode, 23 cm coiled Pt-spring as a counter electrode and catalyst-coated CP as a working electrode enclosed in a glass cell. The electrochemical experiment for HER was studied via CV and LSV at a scan rate of 20 mVs^{-1}. All the potential data were converted into a reversible hydrogen electrode (RHE) scale using the following equation.

$E_{RHE} = E_{Ag/AgCl} + 0.197 + 0.059\ pH$

Where; E_{RHE} is the potential vs RHE; $E_{Ag/AgCl}$ is the potential measure against the Ag/AgCl electrode; 0.197 is the standard Ag/AgCl electrode potential in Volt.

Long-term electrochemical stability of the working electrodes was performed via chronocoulometric measurements at a constant applied voltage of -0.472 V vs RHE for continuous 60000 sec. and 60 run CV cycles at a 20 mVs^{-1} scan rate in an alkaline medium (pH 9.0). Evolved gas samples were analysed via a CIC Dhruv Gas chromatography instrument equipped with a thermal conductivity detector (TCD). A calibration curve was drawn from known standard gas sample mixtures.

Photocatalytic hydrogen generation experiment

The photocatalytic hydrogen production experiments were performed in a 100 mL Pyrex photoreactor at room temperature and atmospheric pressure, and the outlet of the flask was sealed with a silicone rubber septum. In a typical photocatalytic experiment, 5 mg of catalyst was dispersed by constant stirring in 30 mL DI H_2O/ACN (1:1) containing 10 vol% Triethanolamine (TEOA) as the sacrificial electron donor and 0.1 mM Eosin-Y. Before irradiation, the system was bubbled with nitrogen for 30 min to remove the oxygen and ensured that the reaction system was under an anaerobic condition. A 420 W Xe arc lamp (Newport Co., Ltd., USA) with a cut-off filter ($\lambda \geq 420$ nm), which was positioned 10 cm away from the reactor, was used as a light source to trigger the photocatalytic reaction. The evolved gas produced from the upper space above the solution in the reactor was periodically analysed by

sampling for each hour using gas chromatography (Perkin Elmer Clarus 590 GC containing molecular Sieve 5 Å column) with thermal conductivity detector (TCD) using N_2 as carrier gas at periodic time intervals. The volume of the evolved hydrogen was measured by comparing the GC curve generated by 0.1 mL pure H_2 collected at STP. Photostability was tested by analysing the photocatalytic activity of the samples with five consecutive runs at identical conditions. During the experiment, after each cycle, the reactor was evacuated under dark condition and reused in the H_2 generation experiments.

Photoelectrochemical measurements

Photoelectrochemical measurements have been carried out in a three-electrode system using a potentiostat (CH Instruments, CHI 6005E, USA) with an aqueous 0.25 M Na_2SO_4 electrolytic solution using Ag/AgCl saturated with KCl as reference electrode, Pt wire as a counter electrode, and sample loaded modified ITO film as a working electrode. The sample loading over the ITO film with a surface area of 1.5*1.5 cm^2 has been carried out by the dispersion of 5 mg of the sample into 200 µL ethanol and 30 µL of Nafion through ultrasonication and drop cast over the ITO film and dried at RT. The artificial solar simulator of AM 1G illuminator (100 mW cm^{-2}) was used as the light source during the measurement. The electrochemical cell was a conventional three-electrode cell with a 3 mm thick Pyrex glass eyelet. EIS measurements were used to characterize the interfacial properties between the electrode and electrolyte. Nyquist plot at high frequency represents charge transfer process and the diameter of capacitance arc reflects the charge-transfer resistance. The EIS tests were collected under light irradiation at open circuit voltage 0.15 V over a frequency range from 1 to 10^6 Hz. The experimental data were fitted with the Z-view software. In the circuit diagram, R_S represents the series resistance, which includes the resistance of ITO and counter electrode. R_{CT} is the charge-transfer resistance at the photocatalyst interface. It can be interpreted that the large parabola in the high-frequency region indicates higher transportation and exchange resistance from the ITO to the counter electrode. The Mott-Schottky plots were obtained at different frequencies of 1000, 1500, 2000 Hz to determine the flat-band potential.

ECSA (electrochemical specific surface area) value calculation:

The value of electrochemical active surface areas (ECSA) can be measured by determining the electrochemical double layer capacitance (C_{dl}) in non-faradaic region.

$$\text{ECSA} = \frac{C_{dl}}{C_s}$$

Where C_s denotes a specific capacitance value of 0.040 mF/cm^2 depending on the typical reported values.

Apparent quantum yield (AQY) calculation

The apparent quantum yield (AQY) has been measured under the same photoreaction conditions. An optical power/energy meter (Newport, Model: 842-PE) was used to determination of the number of incident photons ($N_{photons}$). The values of $N_{photons}$ and AQY % were calculated using a band-pass filter of 420 nm using the following equations:[6]

$$N_{photon} = \frac{P\lambda t}{hc}$$

Here, P represents the power of the light (0.16 W cm^{-2} = 0.16 J s^{-1} cm^{-2}) in an area of 11.17 cm^2, λ is the wavelength of the light (420 nm), t is the duration of irradiation (4 h), h is the Planck's constant (6.626 x 10^{-34} J s) and c is the velocity of light (3 x 10^8 m s^{-1}).

$$N_{photon} = \frac{0.16 \times 11.17 \times 420 \times 10^{-9} \times 4 \times 3600}{6.626 \times 10^{-34} \times 3 \times 10^8} = 4.92 \times 10^{22}$$

$$AQY\ \% = \frac{2 \times numbers\ of\ evolved\ H_2\ molecule}{numbers\ of\ incident\ photons\ (N_{photon})} \times 100$$

Table S2. Photocatalytic H_2 production of as-synthesized catalyst under visible light irradiation for 4 hrs.

Entry	Catalyst	pH	H_2 activity (μmol g^{-1}h^{-1})	AQY (%)
1	UiO-66-NH_2	9	104	0.25
2	Co-UiO	3	30	0.07
3	Co-UiO	5	137	0.33
4	Co-UiO	9	404	0.98

Table S3. Comparative table of photocatalytic hydrogen production activity.

Photocatalyst	Reaction condition	Condition	SED	H_2 activity	Ref.
Ti_3C_2/TiO_2/UiO-66-NH_2	20 mg photocatalyst, Temp= 5 °C	300 W Xe lamp	Na_2S (0.1M)-Na_2SO_3 (0.1 M) mixed solution (50mL)	1980 μmol g^{-1}h^{-1}	[7]

MoS2/UiO-66-NH_2	0.02 g photocatalyst in 20 mL of various scavengers	300 W Xe arc lamp (λ> 420 nm)	10% methanol	512.9 μmol h^{-1}	[8]
0.5(Co/Zr)-UiO-66-NH_2, 0.5(Ni/Zr)-UiO-66-NH_2, and 0.5(Fe/Zr)-UiO-66-NH_2	50 mg of photocatalyst	300 W Xe arc light	100 mL 15% methanol	29.94 μmol $g^{-1}h^{-1}$	[9]
CD@NH_2−UiO-66/g-C_3N_4 ternary composite	10 mg photocatalyst, Pt (0.8 wt %) as co-catalyst	300 W Xe lamp (λ> 420 nm)	100 ml of sodium ascorbate aqueous solution (5.05 M, pH 6.5)	2.930 mmol$g^{-1}h^{-1}$	[10]
graphene well-wrapped UiO-66-NH_2 octahedrons	5mg samples, 0.05g ErB or RhB and 28μL H_2PtCl_6	300 W Xe lamp (λ> 420 nm)	TEOA and methanol	41.4 mmol$g^{-1}h^{-1}$	[11]
g-C_3N_4/UiO-66-NH_2	50 mg photocatalyst, 1% Pt cocatalyst,	300 W Xe lamp (λ> 420 nm)	100 mL TEOA (10%)	152 μmol $g^{-1}h^{-1}$	[12]
UiO-66 & UiO-66-NH_2	45 mg photocatalyst, water/methanol (3:1) 22.5 mL.	200 W Xe lamp	methanol	2.4 & 2.8 mL	[13]
tetra-decahedral UiO-66- NH_2	5 mg photocatalyst in 25 mL solution, 2 mL water, 20 mL TEOA, 180 mL Acetonitrile	300 W Xe lamp	TEOA	64.06 μmol $g^{-1}h^{-1}$	[14]
Z-scheme UiO-66-NH_2@Au@CdS	10 mg photocatalyst, Pt (0.25 wt%) co-catalyst	300 W Xe lamp (λ> 420 nm)	20 mL L-ascorbic acid (pH=4.0 and 0.1 M)	39.5 μmol $g^{-1}h^{-1}$	[15]
Eosin-Y sensitized UiO-66-NH_2	50 mg photocatalyst, Pt (1 wt%) co-catalyst, Conc.H_2SO_4 3 mL	300 W Xe lamp (λ> 420 nm)	186 mL TEOA (10 vol%)	2760 μmol $g^{-1}h^{-1}$	[16]
Keggin-type polyoxometalates (PW_{12}) PW_{12}@UiO-66-NH_2	20 mg photocatalyst, water/methanol (3:1) 50 mL.	500 W Xe lamp	methanol	72.7 μmol $g^{-1}h^{-1}$	[17]
Pt@UiO-66-NH_2	10 mg photocatalyst, 18 mL Acetonitrile, 0.2 mL DI water	300 W Xe lamp (λ>380 nm)	2 mL TEOA	257.38 μmol $g^{-1}h^{-1}$	[18]
Co-UiO	5 mg catalyst, 30 ml H_2O/CAN (1:1)	420 W Xe lamp (λ> 420 nm)	3 ml TEOA	404 μmol $g^{-1}h^{-1}$	**This work**

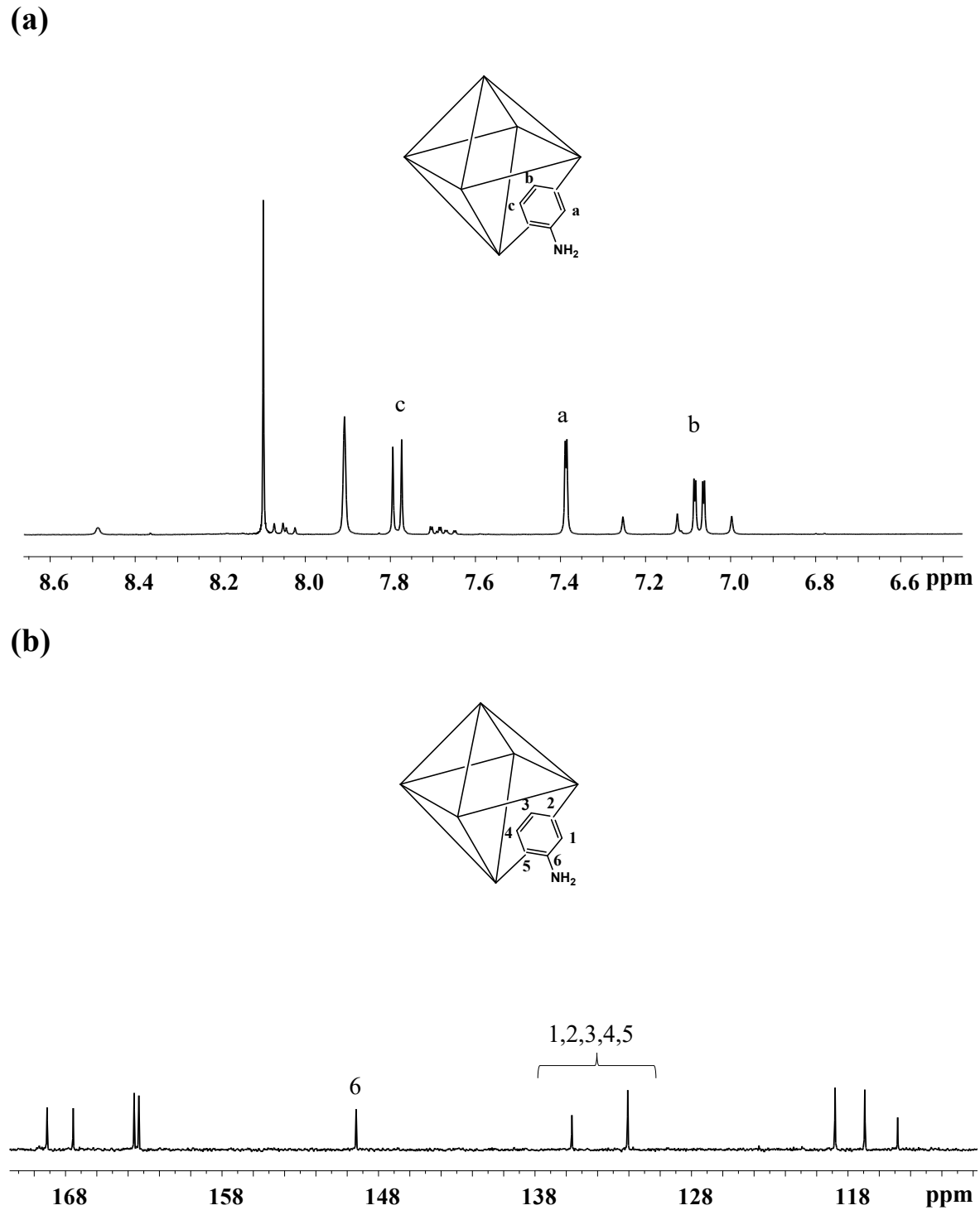

Figure S1. NMR spectra of the UiO-66-NH_2; (a) ^{1}H and (b) ^{13}C in 570 µL of 40% HF solution in DMSO-d_6.

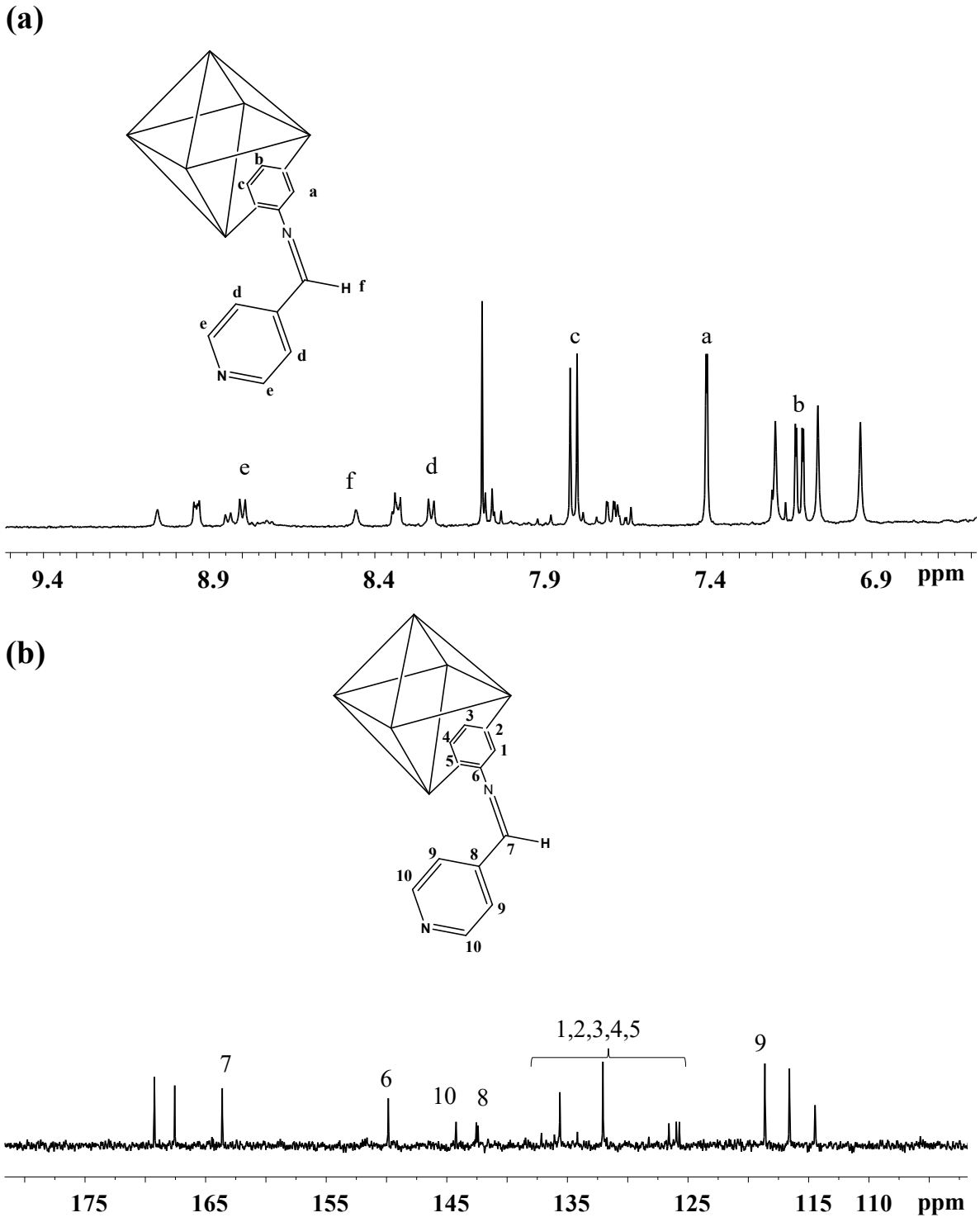

Figure S2. NMR spectra of the UiO-66-N=CH-4-Pyr (A); (a) ^{1}H and (b) ^{13}C in 570 µL of 40% HF solution in DMSO-d_6.

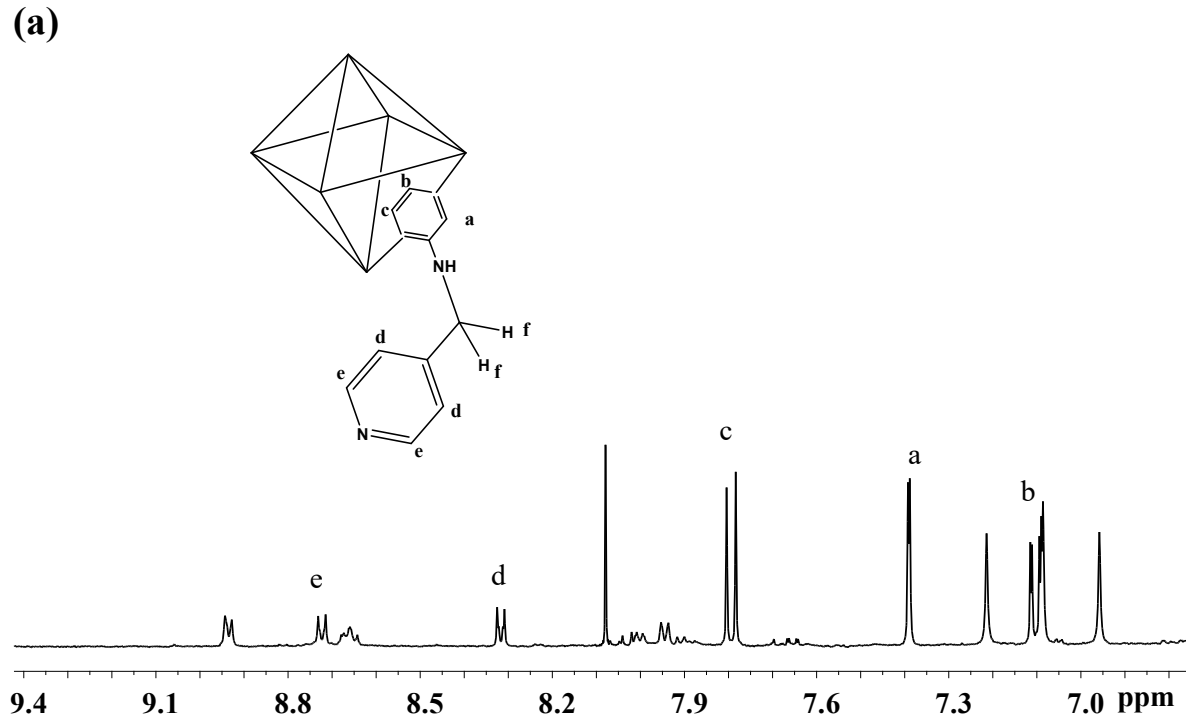

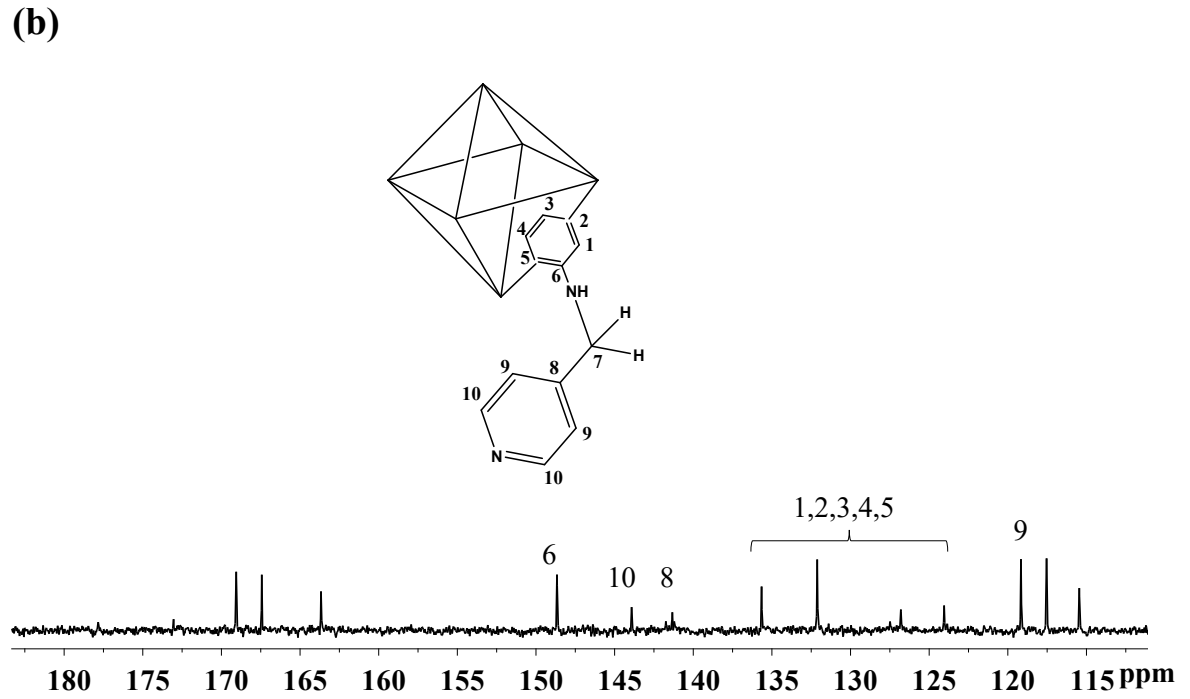

Figure S3. NMR spectra of the UiO-66-NH-CH_2-4-Pyr (A'); (a) ^{1}H and (b) ^{13}C in 570 µL of 40% HF solution in DMSO-d_6.

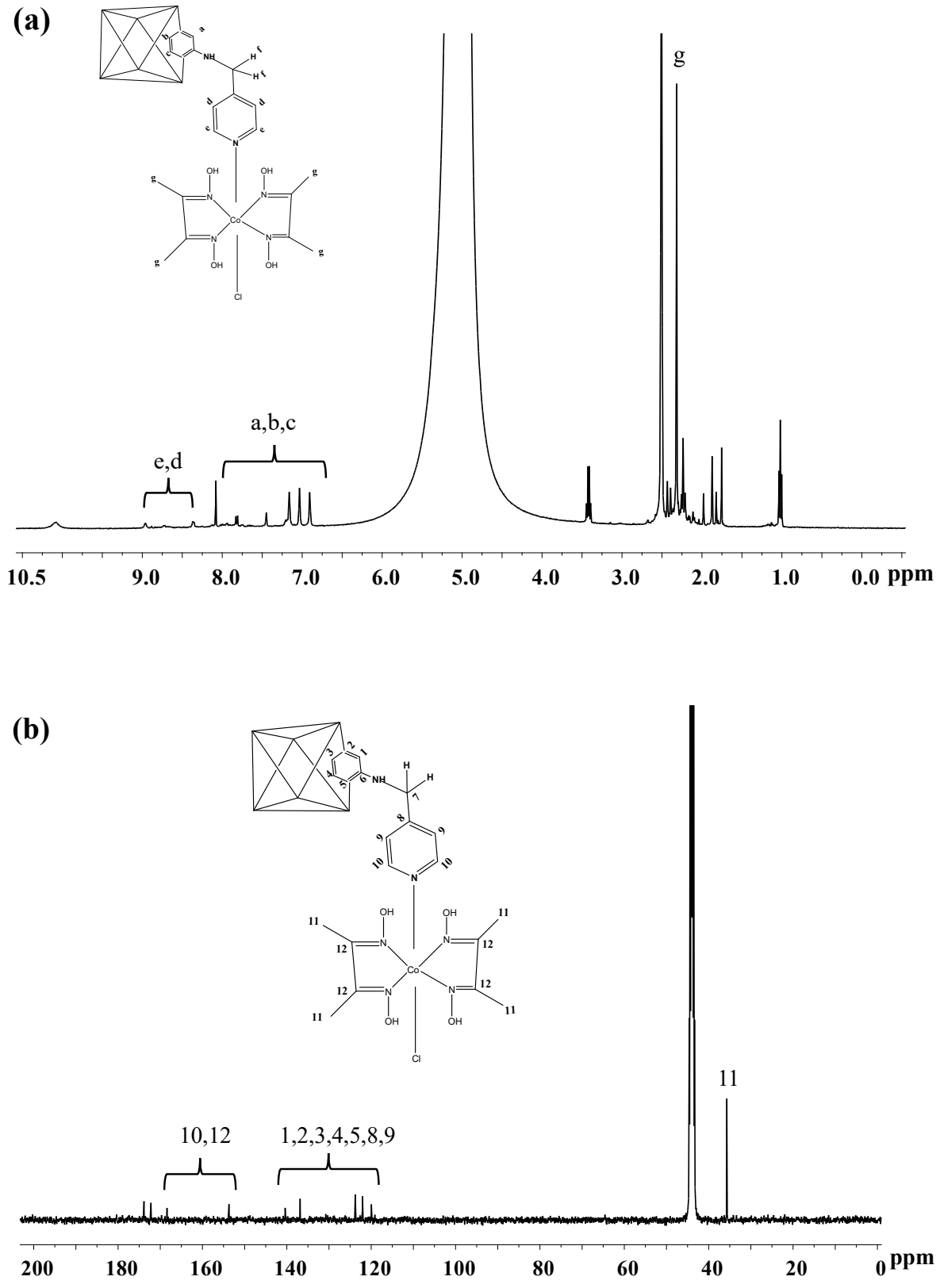

Figure S4. NMR spectra of the Co-UiO; (a) ^{1}H and (b) ^{13}C in 570 µL of 40% HF solution in DMSO-d_6.

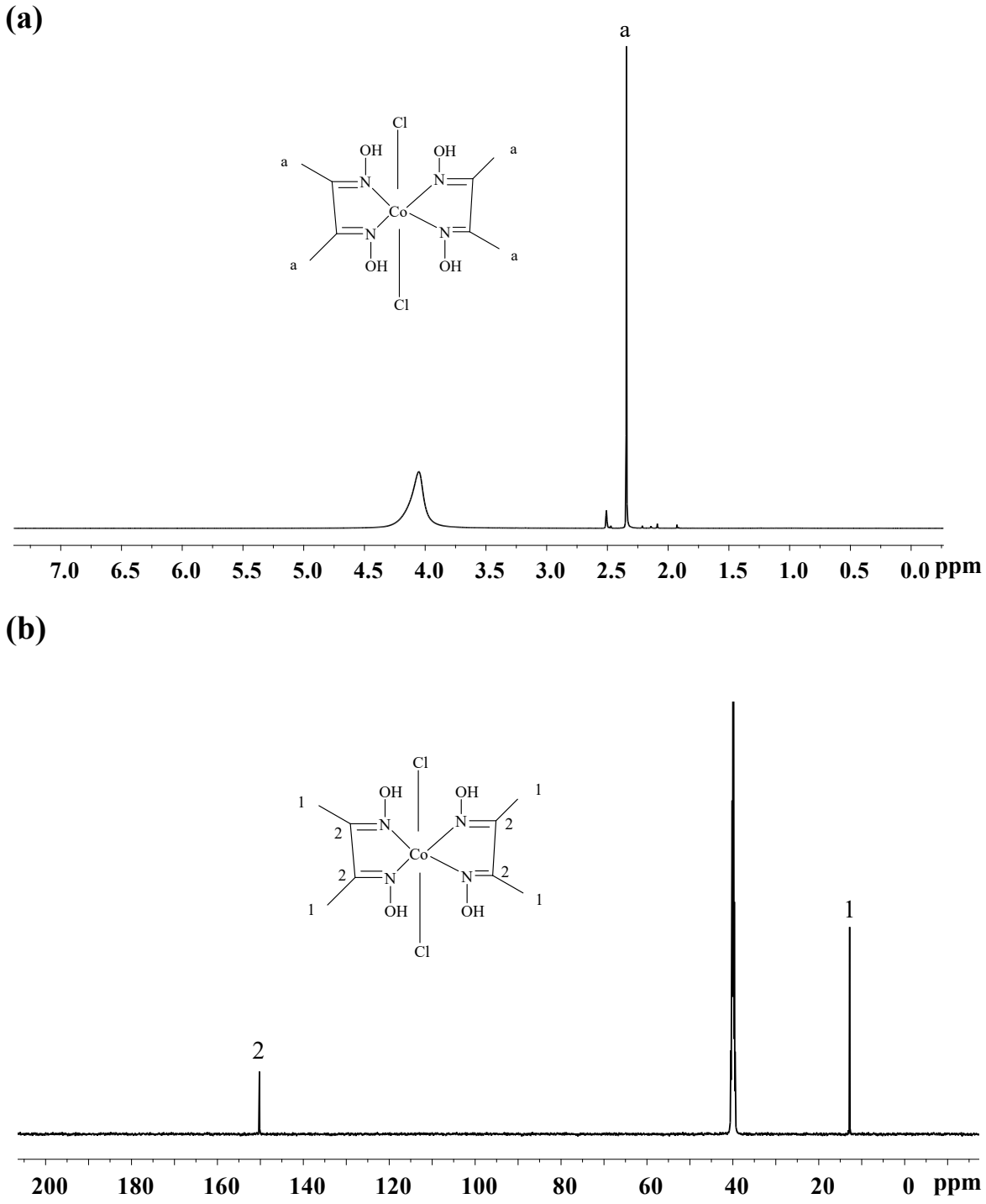

Figure S5. NMR spectra of the Co(dimethylglyoxime)$_2$Cl$_2$; (a) ^{1}H and (b) ^{13}C in DMSO-d$_6$.

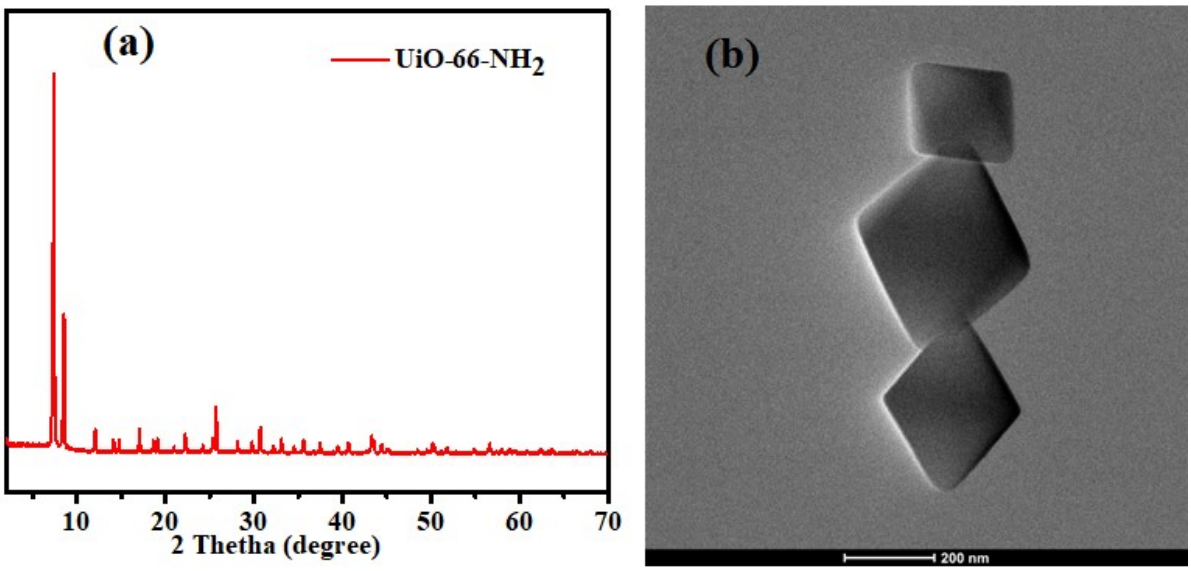

Figure S6. (a) PXRD diffractograms and (b) TEM image of UiO-66-NH_2.

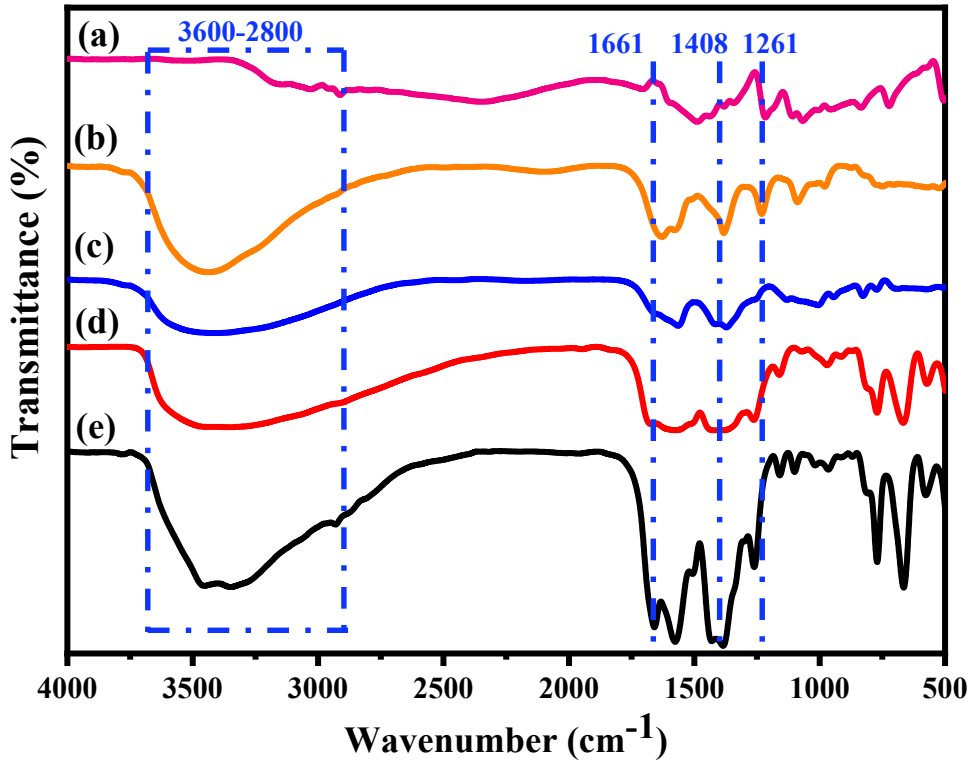

Figure S7. FTIR spectra of the (a) Co(dimethylglyoxime)$_2Cl_2$, (b) Co-UiO, (c) UiO-66-NH-CH_2-4-Pyr, (d) UiO-66-N=CH-4-Pyr, and (e) UiO-66-NH_2.

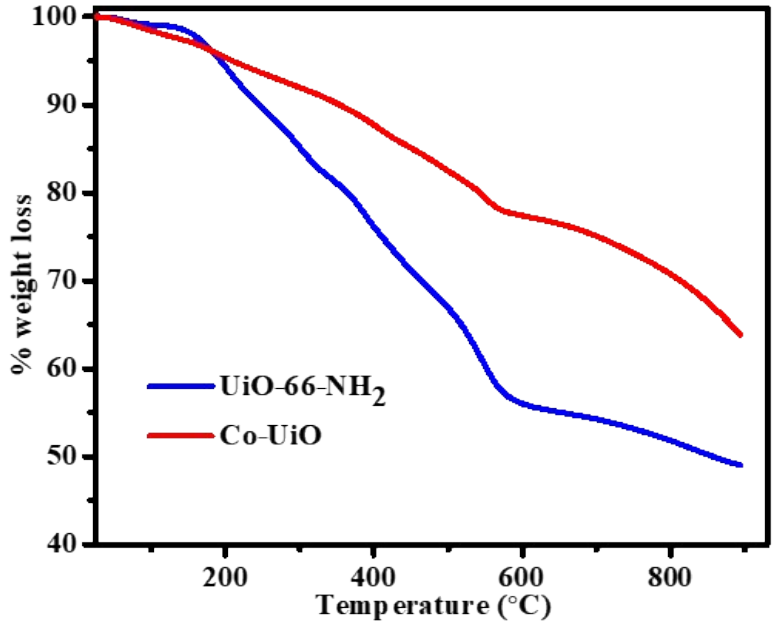

Figure S8. TGA profiles under a flow of N_2 at heating rate of 10 °C min^{-1}.

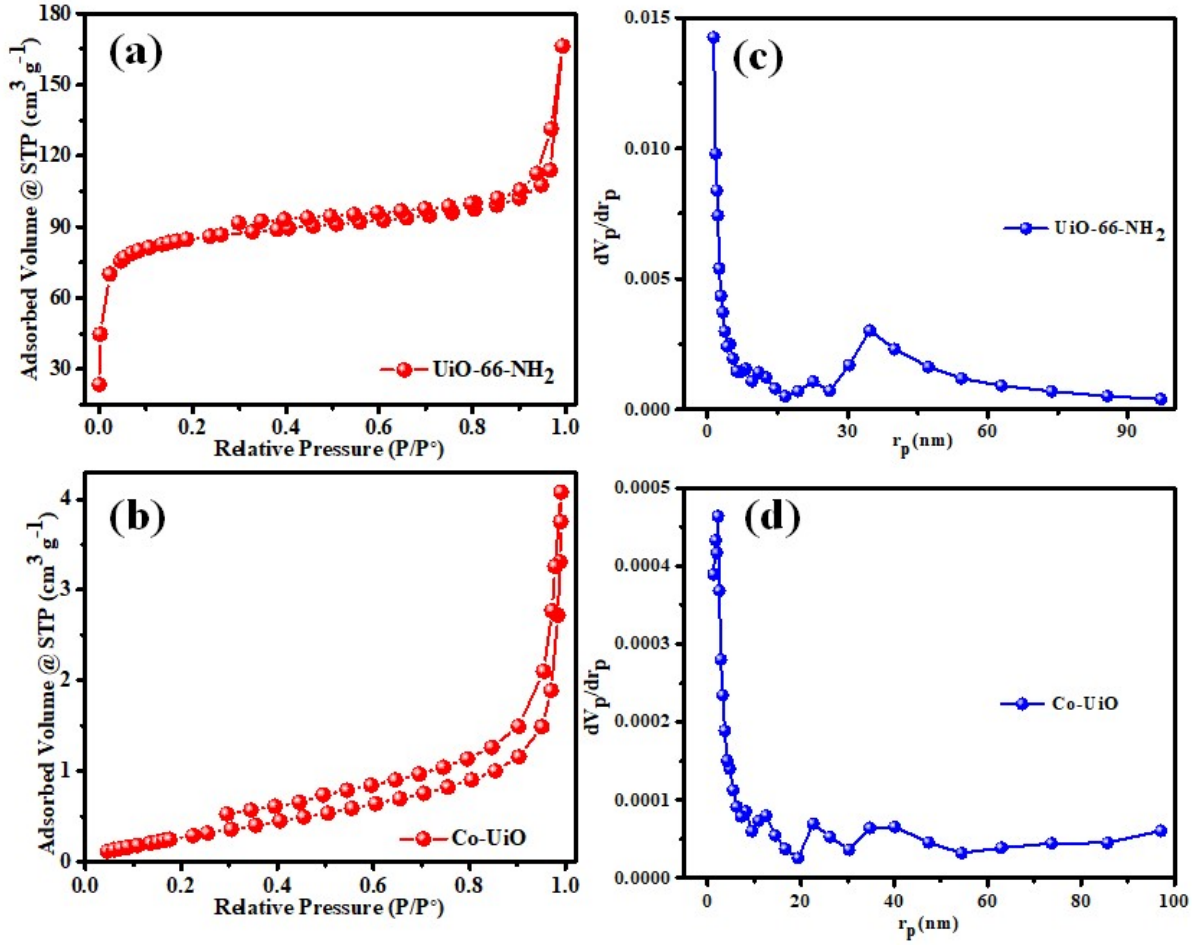

Figure S9. (a, b) N_2 adsorption-desorption isotherms, and (c, d) the corresponding pore size distribution curves of the as-synthesized catalysts.

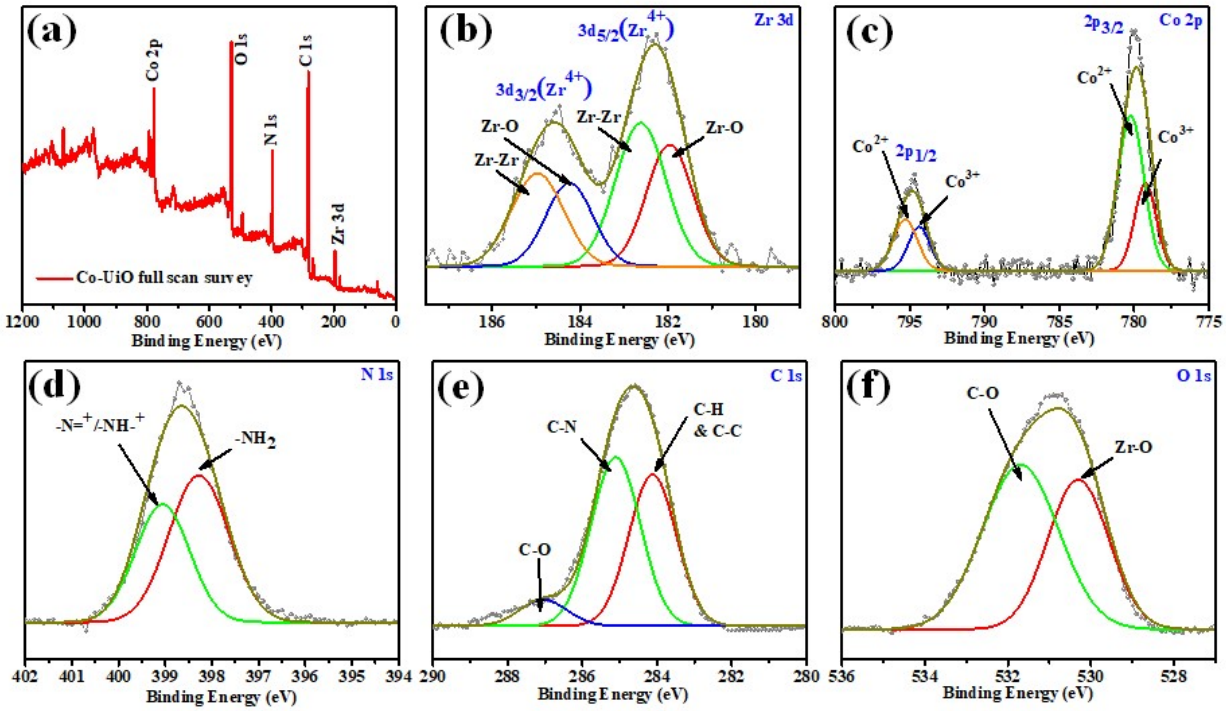

Figure S10. XPS spectra of Co-UiO compound: (a) survey XPS spectrum, (b) Zr 3d, (c) Co 2p, (d) N 1s, (e) C 1s, and (f) O 1s.

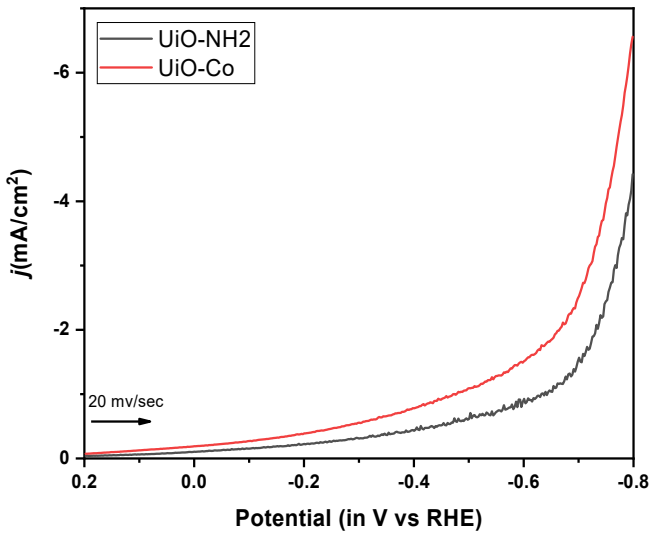

Figure S11. LSV comparison at **pH 8.0** (0.1M CHES buffer) obtained after 20 cycles of CV at 20mv/sec scan rate. Data were recorded at RT with 0.25 cm^2 catalyst modified CP electrodes.

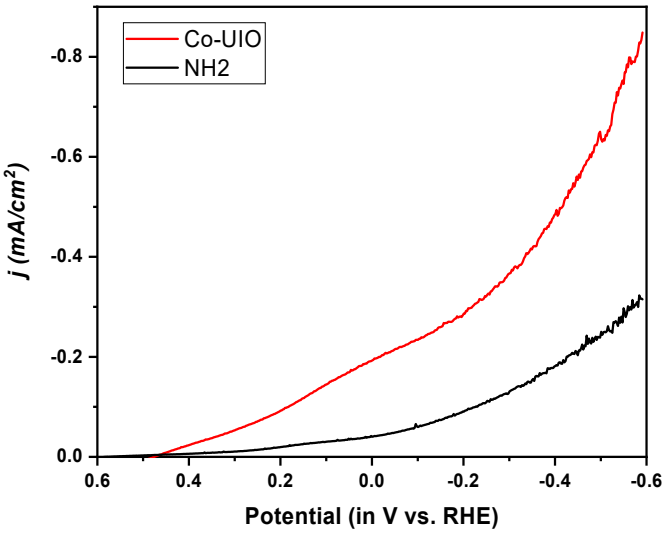

Figure S12. LSV comparison at **pH 7.0** (0.1M CHES buffer) obtained after 20 cycles of CV at 20mv/sec scan rate. Data were recorded at RT with 0.25 cm^2 catalyst modified CP electrodes.

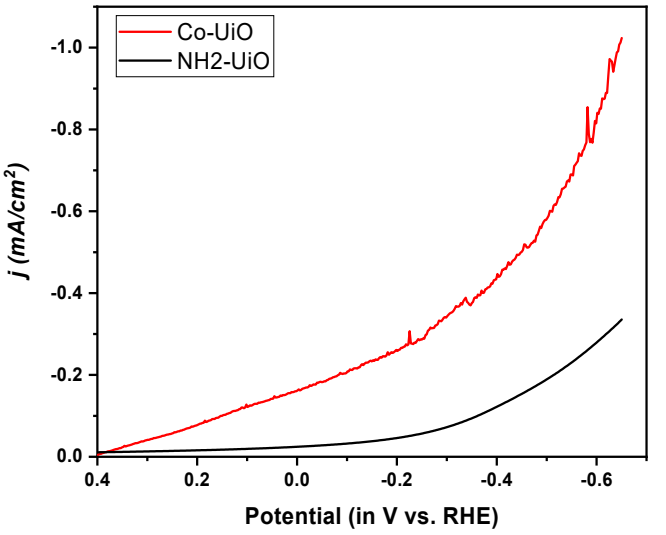

Figure S13. LSV comparison at **pH 9.0** (0.1M CHES buffer) obtained after 20 cycles of CV at 20mv/sec scan rate. Data were recorded at RT with 0.25 cm^2 catalyst modified CP electrodes.

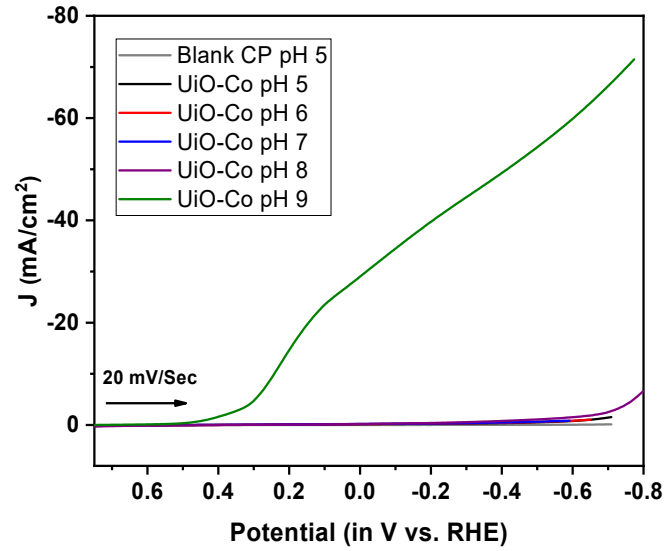

Figure S14. LSV data comparison for UiO-Co at a different pH medium (pH6-9) recorded after 60 cycles CV scan (scan rate 20 mVs-1). Data were recorded at RT with 0.25 cm^2 catalyst modified CP electrodes.

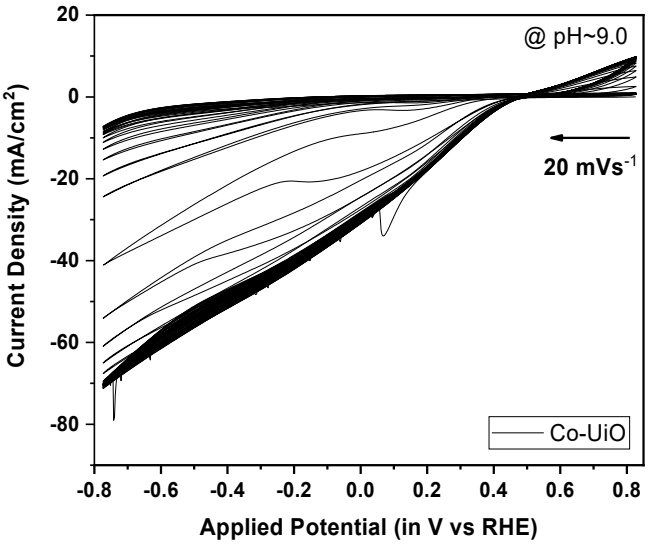

Figure S15. An illustrative figures how CVs of UiO-Co changes with several cycles of CV scans.

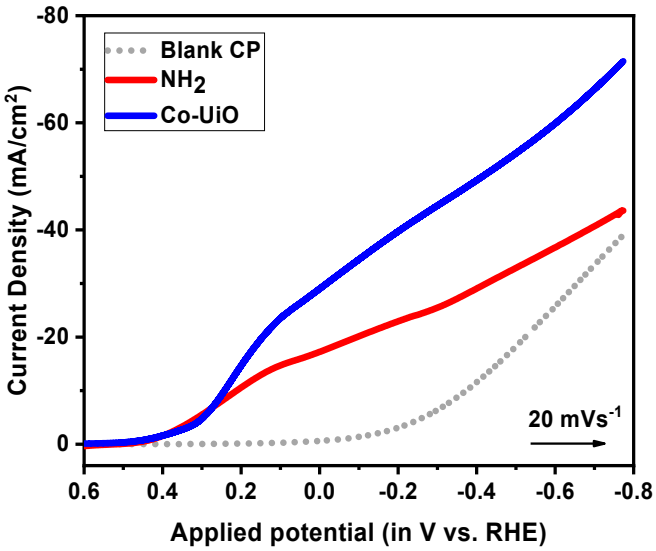

Figure S16. LSV after 60 cycles of CVs, pH 9.0 (0.1M CHES buffer)

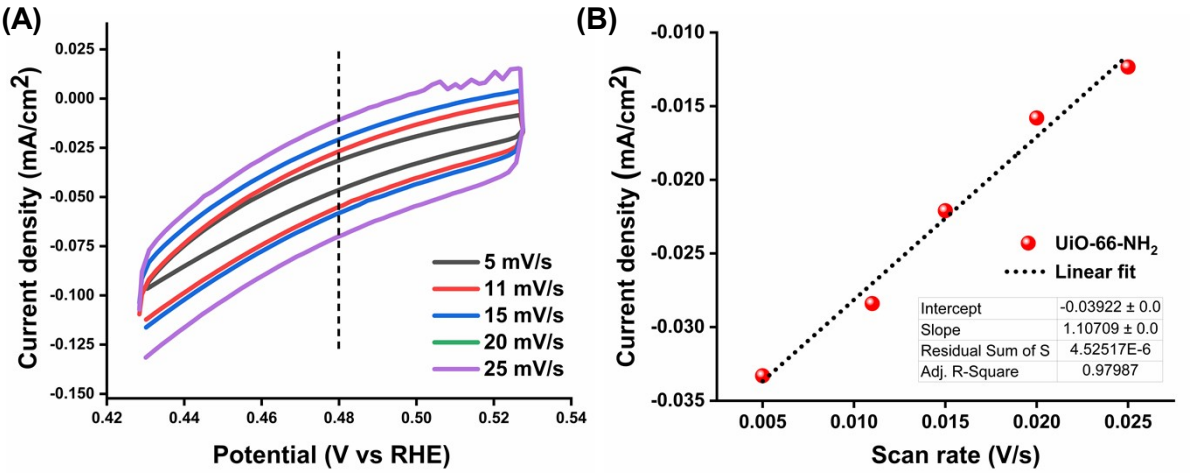

Figure S17. (A) CVs measured at different scan rates from 5 to 25 mV/s for UiO-66-NH_2; (B) Plot of current density at 0.48 volt versus scan rate for UiO-66-NH_2.

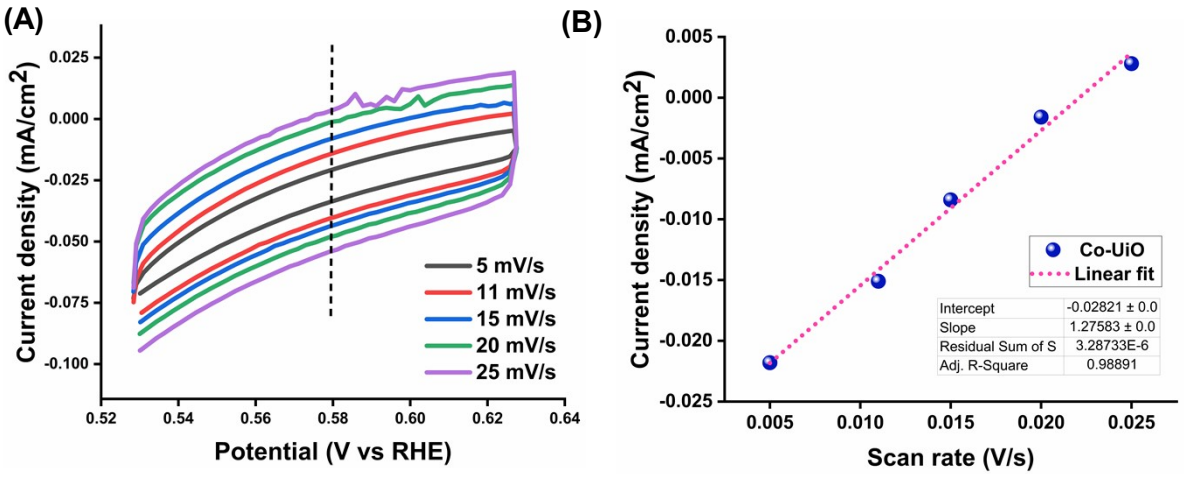

Figure S18. (A) CVs measured at different scan rates from 5 to 25 mV/s for Co-UiO; (B) Plot of current density at 0.58 volt versus scan rate for Co-UiO.

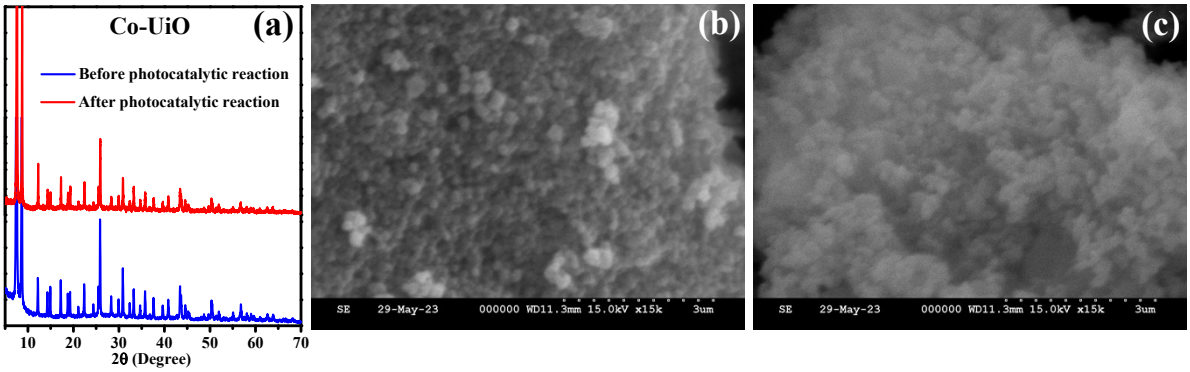

Figure S19. (a) Powder XRD patterns; and SEM images of Co-UiO catalyst [(b) before; (c) after the HER].

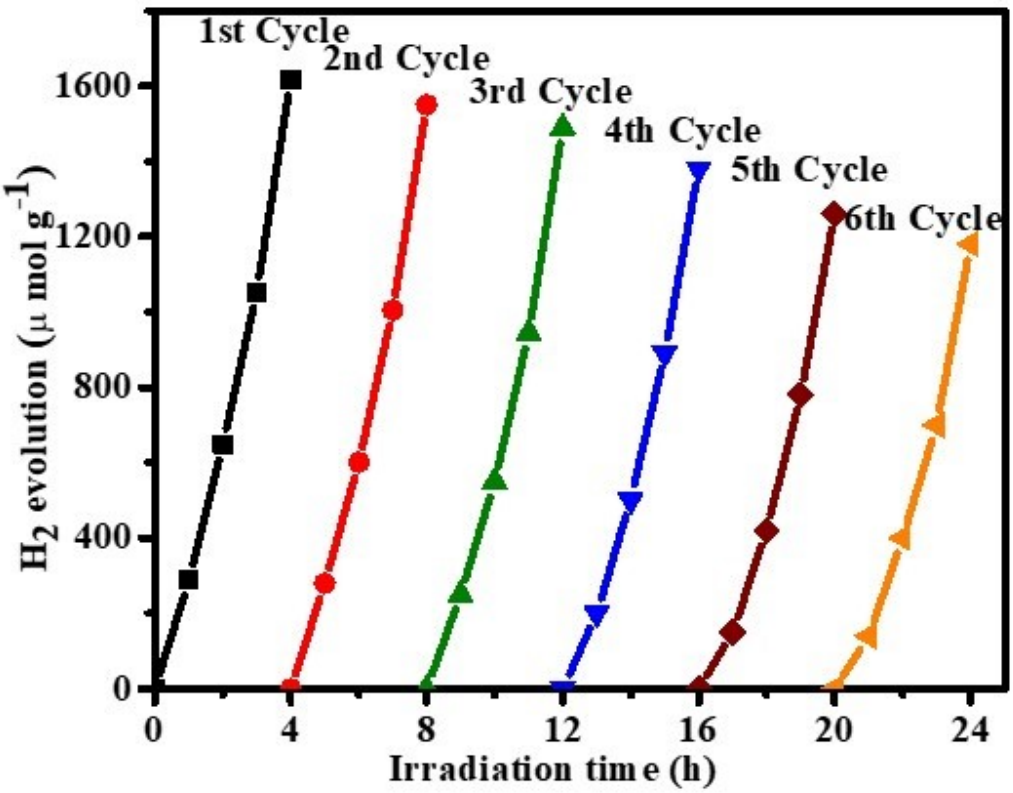

Figure S20. Photo stability test for H_2 production of Co-UiO catalyst under the same reaction condition (irradiation time = 24 h).

Figure S21. Snapshot of the synthesized catalysts.

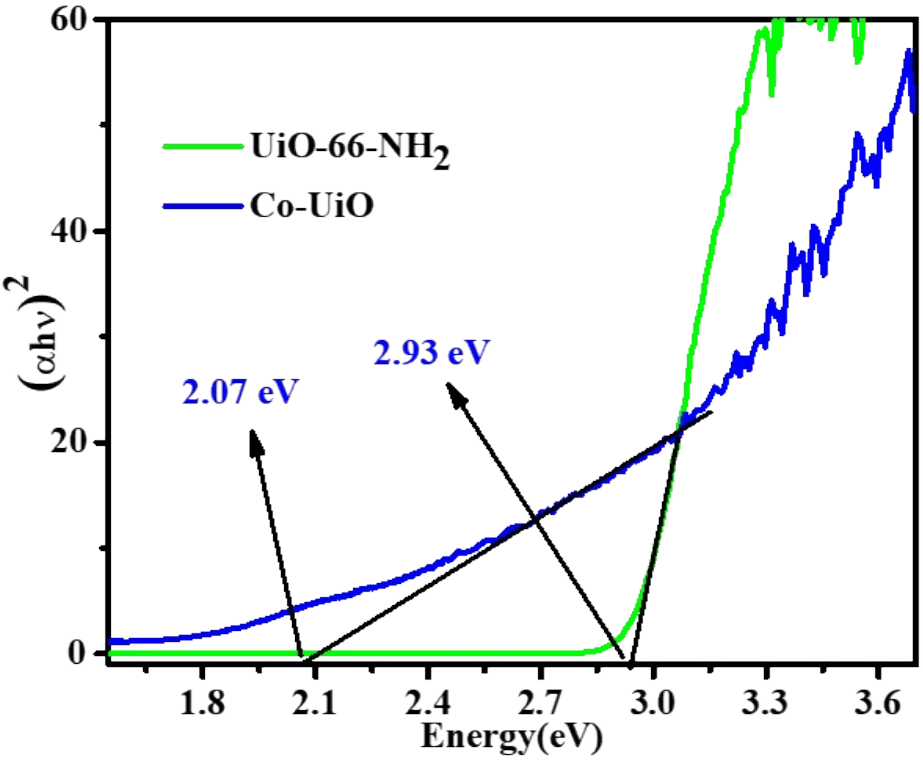

Figure S22. Band gap potentials (Tauc plots) of as-synthesized catalysts.

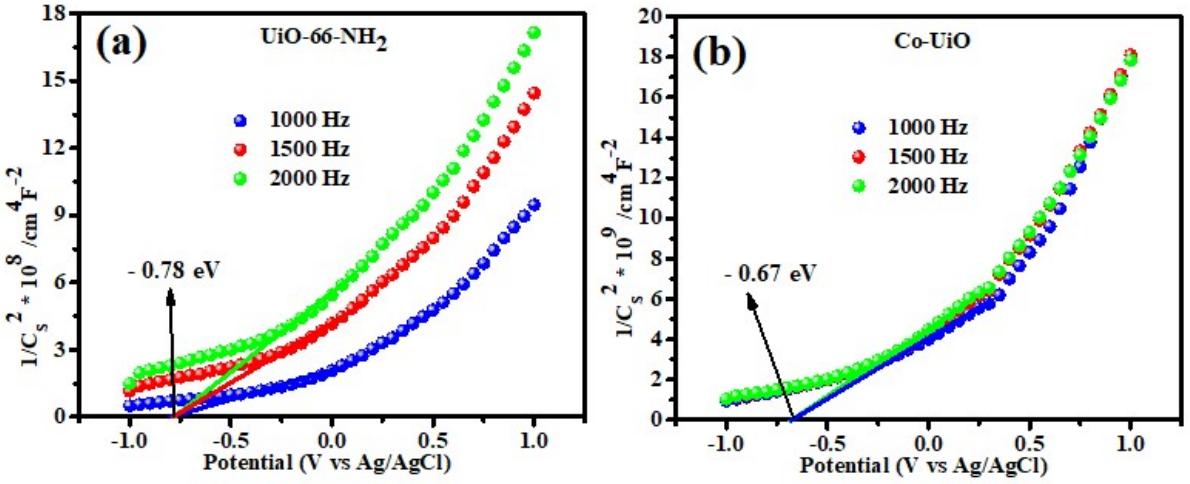

Figure S23. Mott-Schottky plots with different frequencies of (a) UiO-66-NH_2 and (b) Co-UiO catalyst.

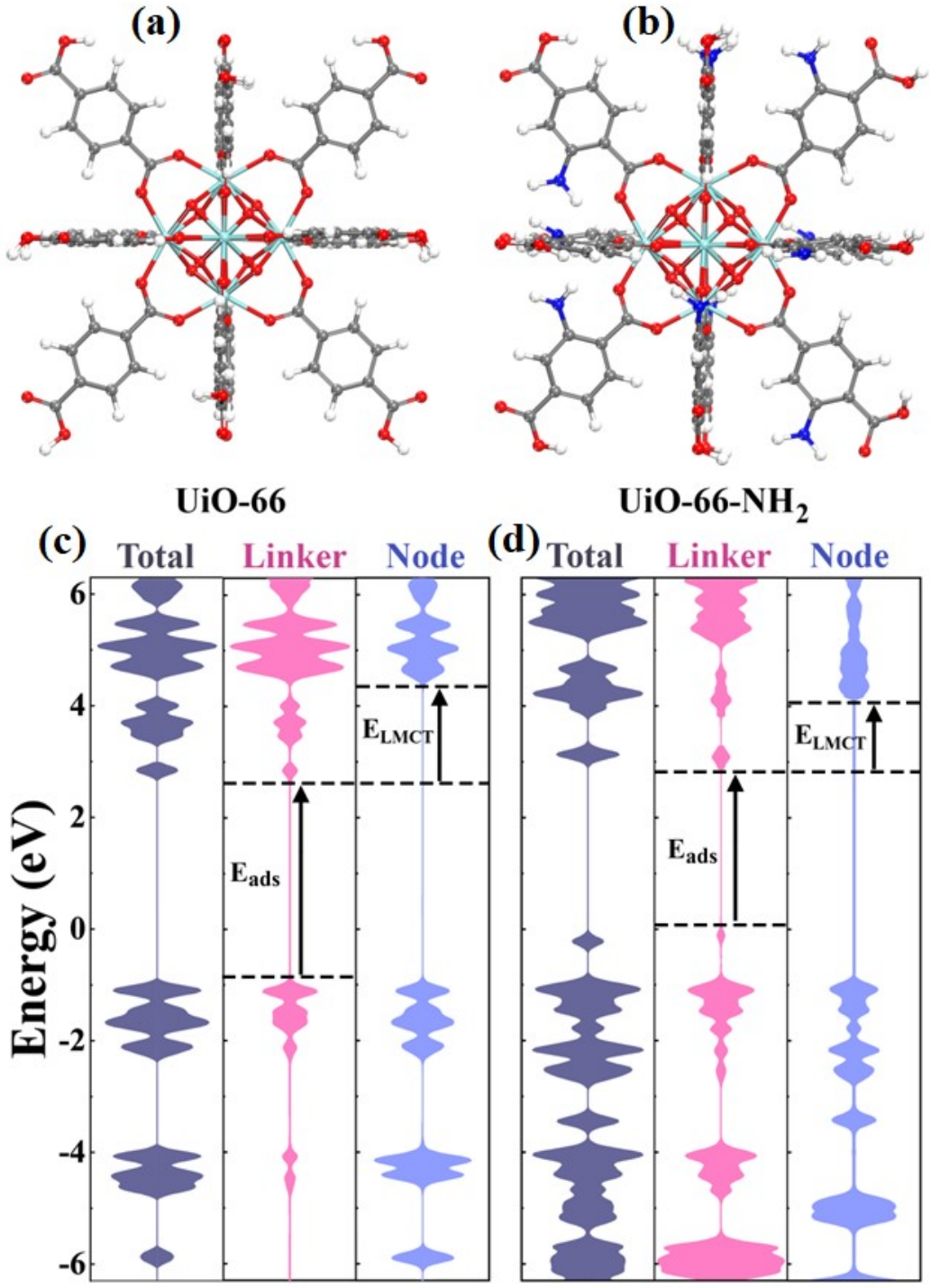

Figure S24. The cluster model of (a) UiO-66 and (b) UiO-66-NH_2 [Here, white, grey, blue, red and cyan colour balls indicate H, C, N, O and Zr atoms, respectively]. Partial density of states of (c) UiO-66 and (d) UiO-66-NH_2. E_{ads} is the energy required to excite the linker E_{LMCT} is the energy required for ligand-to-metal charge transfer process.

References

1. G. N. Schrauzer, G. W. Parshall and E. R. Wonchoba, in *Inorganic Syntheses*, 1968, DOI: https://doi.org/10.1002/9780470132425.ch12, pp. 61-70.
2. J.-D. Xiao, Q. Shang, Y. Xiong, Q. Zhang, Y. Luo, S.-H. Yu and H.-L. Jiang, *Angewandte Chemie International Edition*, 2016, **55**, 9389-9393.
3. F. J. Devlin, J. W. Finley, P. J. Stephens and M. J. Frisch, *The Journal of Physical Chemistry*, 1995, **99**, 16883-16902.
4. M. J. Frisch, *Gaussian 09, revision B.01; Gaussian, Inc.: Wallingford, CT, 2010.*
5. M. D. Hanwell, D. E. Curtis, D. C. Lonie, T. Vandermeersch, E. Zurek and G. R. Hutchison, *Journal of Cheminformatics*, 2012, **4**, 17.
6. S. Sk, A. Tiwari, B. M. Abraham, N. Manwar, V. Perupogu and U. Pal, *International Journal of Hydrogen Energy*, 2021, **46**, 27394-27408.
7. P. Tian, X. He, L. Zhao, W. Li, W. Fang, H. Chen, F. Zhang, Z. Huang and H. Wang, *International Journal of Hydrogen Energy*, 2019, **44**, 788-800.
8. S. Subudhi, G. Swain, S. P. Tripathy and K. Parida, *Inorganic Chemistry*, 2020, **59**, 9824-9837.
9. X. Kong, Q. Pan, S. Song, Z. He, T. Zeng and Y. Yu, *The Journal of Physical Chemistry C*, 2021, **125**, 20320-20330.
10. X. Zhang, H. Dong, X.-J. Sun, D.-D. Yang, J.-L. Sheng, H.-L. Tang, X.-B. Meng and F.-M. Zhang, *ACS Sustainable Chemistry & Engineering*, 2018, **6**, 11563-11569.
11. Y. Wang, Y. Yu, R. Li, H. Liu, W. Zhang, L. Ling, W. Duan and B. Liu, *Journal of Materials Chemistry A*, 2017, **5**, 20136-20140.
12. S. Zhang, K. Chen, W. Peng and J. Huang, *New Journal of Chemistry*, 2020, **44**, 3052-3061.
13. C. Gomes Silva, I. Luz, F. X. Llabrés i Xamena, A. Corma and H. García, *Chemistry – A European Journal*, 2010, **16**, 11133-11138.
14. X. Shi, X. Lian, D. Yang, X. Hu, J. Zhang and X.-H. Bu, *Dalton Transactions*, 2021, **50**, 17953-17959.
15. X. Hou, L. Wu, L. Gu, G. Xu, H. Du and Y. Yuan, *Journal of Materials Science: Materials in Electronics*, 2019, **30**, 5203-5211.
16. J. Shi, F. Chen, L. Hou, G. Li, Y. Li, X. Guan, H. Liu and L. Guo, *Applied Catalysis B: Environmental*, 2021, **280**, 119385.
17. P. Tian, X. He, W. Li, L. Zhao, W. Fang, H. Chen, F. Zhang, W. Zhang and W. Wang, *Journal of Materials Science*, 2018, **53**, 12016-12029.
18. J.-D. Xiao, Q. Shang, Y. Xiong, Q. Zhang, Y. Luo, S.-H. Yu and H.-L. Jiang, 2016, **55**, 9389-9393.